Available online at www.sciencedirect.com
SCIENCE DIRECT®
Journal of Chromatography A, 1021 (2003) 93–104
JOURNAL OF CHROMATOGRAPHY A
www.elsevier.com/locate/chroma

Mechanism and kinetics of protein transport in chromatographic media studied by confocal laser scanning microscopy
Part I. The interplay of sorbent structure and fluid phase conditions

Jürgen Hubbuch [a,*], Thomas Linden [b], Esther Knieps [a], Anders Ljunglöf [c], Jörg Thömmes [d], Maria-Regina Kula [a]

[a] *Institut für Enzymtechnologie, Heinrich-Heine Universität Düsseldorf, Jülich 52426, Germany*
[b] *Merck & Co. Inc., Vaccine Bioprocess R & D, Sumneytown Pike, West Point, PA 19486-0004, USA*
[c] *Amersham Biosciences AB, Björkgatan 30, Uppsala SE-751 84, Sweden*
[d] *IDEC Pharmaceuticals Corporation, 11011 Torreyana Road, San Diego, CA 92121, USA*

Received 25 March 2003; received in revised form 31 July 2003; accepted 29 August 2003

Abstract

An experimental study on the interplay of sorbent structure and fluid phase conditions (pH) has been carried out examining adsorption and transport of bovine serum albumin (BSA) and a monoclonal antibody (IgG 2a) on SP Sepharose™ Fast Flow and SP Sepharose™ XL. SP Sepharose™ Fast Flow is characterised by a relatively open pore network, while SP Sepharose™ XL is a composite structure with ligand-carrying dextran chains filling the pore space. Both adsorbents have similar ionic capacity. Protein transport and adsorption profiles were evaluated using confocal laser scanning microscopy. Under all investigated conditions, BSA uptake could be adequately explained by a pore diffusion mechanism. The adsorption profiles obtained for IgG 2a, however, indicated that changes in fluid phase conditions as well as a change in the solid phase structure could result in a more complex uptake mechanism as compared to pore diffusion alone. This mechanism results in a fast transport of proteins into the adsorbent, followed by an overshoot of protein in the center of the sorbent and a setback towards a homogeneous adsorption profile.

Keywords: Confocal laser scanning microscopy; Adsorption profile; Composite media; Protein transport; Proteins

1. Introduction

Ion exchange chromatography has historically been one of the most commonly employed techniques in the downstream processing of biological molecules within the pharmaceutical and biotech industry [1]. In order to optimise its performance for a given task a wide variety of different chromatographic resins is currently commercially available ranging from high-resolution media for analytical HPLC to preparative media allowing the application of highly complex feed solutions. These adsorbents differ in size, porous structure and surface architecture leading to significant changes in protein uptake rate, accessibility of the pores for molecules of different size and available capacity for a given target [2].

Recently there is an increasing interest in the design of more advanced adsorbent structures, trying to achieve different mass transfer characteristics and optimise the available surface area for protein binding and thus tailoring the solid phase for specific applications. Among these new adsorbent types are the so-called composite media. These adsorbents consist of a rigid porous base matrix filled with a ligand-carrying phase consisting of organic polymers. The porous base structure provides the stability required for packed bed applications, while the polymer phase yields a binding space of high ligand density and accessibility. In a detailed study investigating the protein adsorption characteristics of a composite resin consisting of a porous silica base matrix filled with polyacrylamide it was found that this adsorbent structure provides a significant higher capacity

* Corresponding author. Tel.: +49-2461614173; fax: +49-2461612490.
E-mail address: j.hubbuch@fz-juelich.de (J. Hubbuch).

0021-9673/$ – see front matter © 2003 Elsevier B.V. All rights reserved.
doi:10.1016/j.chroma.2003.08.112

than conventional supports. Furthermore, the intra-particle transport rates were determined to be higher than predicted for transport based on pore diffusion mechanisms [3–6]. The high capacity of these adsorbents was predominantly due to protein binding in the polymer gel phase. A correlation of the surface area exhibited by the base matrix of such a sorbent and the surface area required to accommodate the protein bound at equilibrium revealed that most of the adsorption takes place within the functionalised hydrogel [5]. The fast intra-particle transport was explained by a shift from a pore diffusion mechanism as found for macro-porous adsorbents to a transport mode based on a so-called homogeneous diffusion [5].

Data on protein adsorption and transport are traditionally limited to kinetic adsorption studies employing finite bath or frontal analysis where the amount of adsorbed protein is measured indirectly by the depletion of protein in the fluid phase followed by an interpretation of the obtained dependencies employing a multiplicity of mathematical models [6–9]. It was, however, pointed out by Chang and Lenhoff [10] that reasonable fits to a single experimental data-set could be obtained by using both pore diffusion as well as homogeneous diffusion models. Therefore the actual physical events within the adsorbent cannot be discriminated. The experimental verification of the real events—mode of transport and adsorption profiles—within the porous resin for a given set of conditions is therefore an inevitable prerequisite for understanding, modelling, and utilisation of adsorption and transport phenomena.

A solution to this lack of information is currently arising in a method employing confocal laser scanning microscopy (CLSM), allowing the detection of proteins labelled with fluorescent dyes within porous adsorbents. The feasibility of this technique to examine adsorption processes has already been shown in studies examining adsorption profiles of Protein A on IgG Sepharose^{TM} 6 Fast Flow or lysozyme and human IgG on cation exchangers [11,12]. By combining this method with batch uptake experiments traditionally used for adsorption studies it is now possible to obtain not only the classical fluid phase information but also simultaneously to detect the intra-particle adsorption profile over time [12,13].

In earlier studies, the adsorption of BSA and monoclonal IgG on SP Sepharose^{TM} Fast Flow under various conditions has been particularly investigated [14]. It was found that at low ionic strength BSA adsorption could be described well by the classical ‘shrinking core’ behaviour. The protein molecules first saturated the outer shell of the support resulting in a sharp adsorption profile moving towards the center of the support. At low ionic strength, i.e. strong protein–matrix interactions, protein adsorption resulted in a sharp adsorption profile and molecules bound to the matrix remained at their initial binding place, while newly arriving proteins were transported past the adsorbed protein layer saturating the adsorbent shell by shell. With increasing ionic strength, i.e. weaker protein–matrix interactions, desorption of initially bound protein molecules occurred and further transport towards the particle center could be observed. Furthermore, during IgG adsorption, a significant change in adsorption pattern could be detected with a change in fluid phase conditions, i.e. a shift of pH from 4.5 to 5.0. The resulting shift in protein surface properties led to a situation where initially bound protein is further transported towards the center of the support, while newly arriving molecules bind to the outer rim of the support. These experimental conditions resulted further in a drastic increase of the overall uptake rate and faster saturation of the support as compared to classical pore diffusion observed for BSA. During investigations employing a micro-column—which allows detailed studies of dynamic processes within an adsorbent particle—it was possible to resolve the adsorption profiles associated with these high uptake rates. [15]. The resulting adsorption profiles resemble a wave of molecules building up towards the centre, thus leading to an overshoot of adsorbed protein, followed by a return towards a homogeneous protein distribution over the cross sectional area of the support. Mechanistic explanations of these phenomena have been given by Liapis et al. [16], Grimes and Liapis [17] and Dziennik et al. [18]. In another approach, it was shown by Martin et al. [19] that a similar adsorption pattern could be obtained with existing model descriptions when accounting for impurities in the investigated protein solutions. During the experimental studies mentioned above, the fast saturation of the support could be linked to a change of protein surface properties resulting from a change of mobile phase conditions. In this paper, we extend the above studies investigating the effect of the stationary phase by a detailed analysis of the adsorption behaviour of BSA and IgG on SP Sepharose^{TM} XL and Sepharose^{TM} FF. Sepharose^{TM} XL is a composite adsorbent, where dextran chains are grafted to the agarose backbone and derivatised with sulfo propyl groups [20]. This adsorbent architecture results in a substantially increase of the accessibility of the ligand-carrying layer, and thus might result in a possible impact of matrix surface properties on the transport mode.

2. Material and methods

2.1. Adsorbents, proteins and chemicals

Bovine Serum Albumin (BSA) with a purity of >98% was ordered from Sigma Aldrich (Deisenhofen, Germany). The IgG 2a was a gift from Boehringer Ingelheim Pharma (Ingelheim, Germany). Mono-functional dyes Cy3 and Cy5 were obtained from Amersham Biosciences (Uppsala, Sweden) and Alexa 488^{TM} from Molecular Probes (Leiden, The Netherlands). The chromatographic resins SP Sepharose^{TM} Fast Flow and SP Sepharose^{TM} XL and all other chromatographic resins employed during this work were obtained from Amersham Biosciences (Uppsala, Sweden). The resins were size fractionated for confocal studies with a lower and upper limit of 80 and 100 μm, respectively. Dextran

standards of various molecular weights were purchased from Pharmacosmos (Viby, Denmark). Sodium acetate (p.a.), sodium chloride (p.a.) and sodium hydrogen carbonate (p.a.) were purchased from Merck (Darmstadt, Germany); all other chemicals from Roth (Karlsruhe, Germany).

2.2. Finite bath experiments

Adsorbent capacity for various fluid phase conditions was determined employing finite bath adsorption experiments. All experiments were carried out using 50 mM acetate buffer at pH 4.5 and 5.0. A known amount of adsorbent (suction dried) was added to the respective buffer solutions resulting in an 1:10 w/w slurry. Known volumes of this slurry were added to several tubes containing a protein solution of defined concentration and volume. The protein-adsorbent suspension was than incubated for 24 h in an over-head shaker. The remaining protein concentration in the liquid phase was then determined employing UV 280 measurements. The data obtained from these finite bath adsorption experiments was evaluated employing the Langmuir isotherm given in Eq. (1):

$$Q^* = Q_{\max} \frac{C^*}{k_d + C^*} \quad (1)$$

Where Q^* represents the amount adsorbed to the support at equilibrium with the fluid phase having a concentration C^*. $Q_{\max}$ is the maximum capacity of the support for the conditions investigated and k_d the dissociation constant.

Studies of adsorption kinetics were then carried out in a batch adsorption reactor equipped with an overhead mixing device. Fifty microlitres of a defined protein/adsorber suspension (0.94 mg/ml/0.15 g) were incubated at room temperature. The decrease of protein concentration in the liquid phase was determined at regular intervals by taking samples of 120 μl from the reactor followed by centrifugation of the adsorbent in the liquid phase and evaluation of the protein concentration in the liquid phase using UV 280 measurements.

All adsorption studies have been determined with native (unlabelled) protein. In previous studies no significant influence of the labelling procedure or the label itself has been detected for the systems studied in this work [26].

2.3. Labelling and preparation of protein solutions

Labelling of the protein was carried out according to the standard procedures recommended by the manufacturers. The degree of labelling (DOL) was determined as 0.6–0.8 for BSA and 0.4 for IgG 2a. The obtained protein solutions were further diluted by a factor 1:20 with un-labelled protein. This procedure enables us to clearly differentiate between signals of the highly diluted labelled protein in the bulk solution and the high intensity of the emitted light from highly accumulated (liquid phase) or adsorbed (solid phase) and therefore concentrated proteins.

2.4. Determination of size exclusion distribution coefficients

The determination of the distribution coefficient was carried out in an appropriately packed XK 16/70 column employing an FPLC^{TM} system equipped with an UV-1 monitor (Amersham Biosciences, Uppsala) and a Shimazu RID-6A refractive index detector. The experimental procedure was carried out according to Hagel [21]. Prior to a chromatographic run, more than 2 column volumes (CV) of the mobile phase (50 mM sodium acetate pH 4.5) were used for equilibration. In experiments investigating the distribution coefficient of the adsorbents previously saturated with BSA, we employed a 10 mg/ml BSA solution (in equilibration buffer) until a breakthrough of 90% was reached. The distribution coefficients, K_D, were determined using dextran standards of different molecular mass ranging from 1.08 to 401.3 kg/mole. The distribution coefficients were calculated according to Eq. (2) [21,22]:

$$K_D = \frac{(V_R - V_0)}{V_P} = \frac{(V_R - V_0)}{(V_t - V_0)} \quad (2)$$

where V_R is the retention volume, V_0 the void volume, V_P the pore volume and V_t the total liquid volume of the column.

2.5. Detection of confocal images

Confocal images were detected employing a LSM510 Zeiss confocal laser scanning microscope. The microscope was equipped with separate pinholes for the investigated emission wavelengths and the two objective lenses Plan-Neofluar 40x/1.3 Oil and C-Apochromat 63x/1.2Wcorr were used. Multi-component scans were carried out in a sequential scan mode employing the following wavelength settings: Alexa 488^{TM} (Ex.: 488 nm; Em.: 505–530 nm), Cy3 (Ex.: 543 nm; Em.: 560–615 nm) and Cy5 (Ex.: 633 nm; Em.: LP 650 nm). Suitable laser intensity has been chosen in order to reduce effects resulting from photo-bleaching, i.e. less than 5% [15]. The scans over the cross sectional area of the supports within the micro-column were carried out along the optical *x–y* axis, i.e. horizontally. A prerequisite for a correct evaluation of the amount of adsorbed protein within a support is that the analysed scan represents the cross sectional area (CSA) through the centre point of the adsorbent. For supports with known diameter, this prerequisite can be easily fulfilled by focussing on the CSA with the respective diameter. For commercially available supports, which exhibit a certain size distribution, the middle plane was found by a simple procedure prior to an experimental run [15]. The integrity of the signal over the cross sectional area—reflection of light due to the adsorbent material–has been checked prior to an experimental run by *z*-scans through a saturated adsorbent. In order to account for the intensity scattering on the outer rim of the support—which might influence the correct estimation of the overall intensity—the following procedure was followed. Prior to

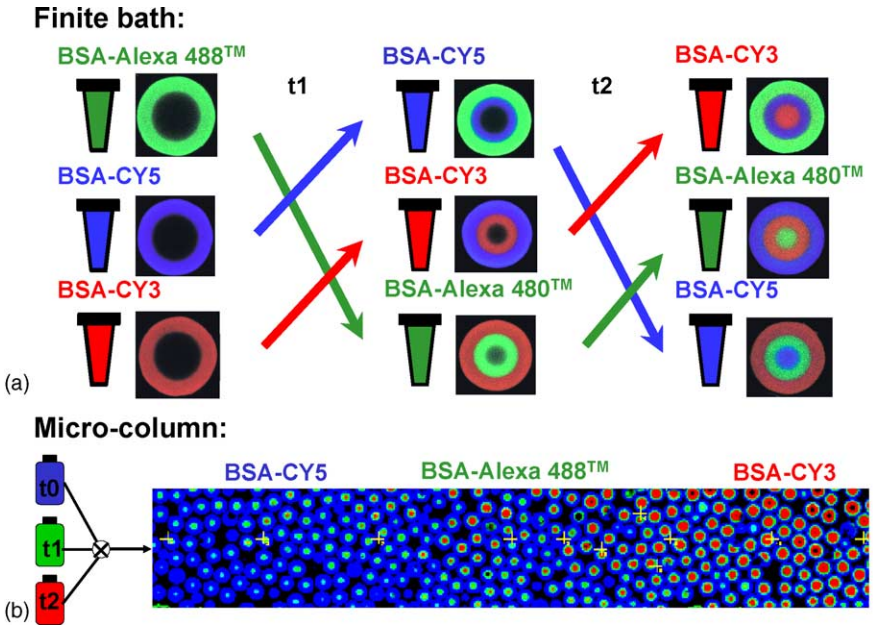

Fig. 1. Principles of the multi-dye method during finite bath and micro-column experiments. (a) Adsorber are incubated with differently labelled but otherwise identical protein solutions in three finite bath reactors. At time t_1 and t_2 the respective supernatants are switched according to the arrows indicated in the figure. (b) The feed to the column is switched from differently labelled but otherwise identical protein solutions at time t_1 and t_2.

the respective adsorption studies a picture of the empty adsorbent was taken to determine its exact size. When analysing the respective intensity profiles, the exact particle dimensions where determined by simply overlaying the picture of the 'empty adsorbent' with the fluorescent profiles.

2.6. Multi-dye method

The change of protein positioning over time during the adsorption process was evaluated using the methodology of a multi-dye method developed by Linden et al. [14] for batch incubations. The method is based on the consecutive incubation of adsorbent particles with differently labelled but otherwise identical protein solutions. To ensure a continuity of the fluid phase conditions during batch adsorption studies three finite bath incubations with differently labelled but otherwise identical protein composition are performed simultaneously (see Fig. 1). In detail, three 2 ml tubes were each filled with 1.5 ml of protein solution with a total protein concentration of ~2.5 mg/ml and each solution consisting of a 1:10 ratio of labelled protein conjugate and the unlabelled species. A defined volume of an 1:3 (w/w) slurry was added. For confocal analysis samples of 0.007 ml were taken from the tubes. After defined incubation times the batches were centrifuged (30 s; 14,000 × g) and the supernatant quantitatively exchanged employing a pattern which ensures that each supernatant is used only one single time for a specific tube (see arrows in Fig. 1) [14]. Employing such a sequential exchange pattern of the supernatants of the three incubators ensures a consistent protein concentration in the incubation reactor and allows conclusions about a change of adsorption sites over time of the respective protein fractions while the sum of the fluorescence intensities representing the net adsorption profiles.

During our study it became evident, however, that a detailed investigation of rapid changes within the adsorbent requires a method with a lower or no time delay caused by experimental handling. In the present study, investigations where experimental handling showed to be a limiting factor were therefore carried out employing a micro-column [15] and simply switching between three differently labelled-Cy3, Cy5 and Alexa™ 488— but otherwise identical feedstocks of BSA or IgG 2a during a chromatographic breakthrough experiment (see Fig. 1).

3. Results and discussion

3.1. Structural characterisation

The two adsorbents investigated in this study (i.e. SP Sepharose™ Fast Flow and SP Sepharose™ XL) are based on porous 6% cross-linked agarose (average diameter 9 × 10^{-5} m), and have the same ionic capacity (~200 μmol Na^+/ml). SP Sepharose™ Fast Flow is characterised by a relatively open pore network with the ligands attached to the pore walls. On SP Sepharose™ XL, dextran has been grafted to the agarose backbone before coupling of sulphopropyl groups. This procedure basically fills the pores of the agarose with a ligand-carrying network.

A comparison of the distribution coefficients K_D for various molecular weight standards obtained for SP Sepharose™ Fast Flow and SP Sepharose™ XL shows distinct differences between the two adsorbents. From Fig. 2a

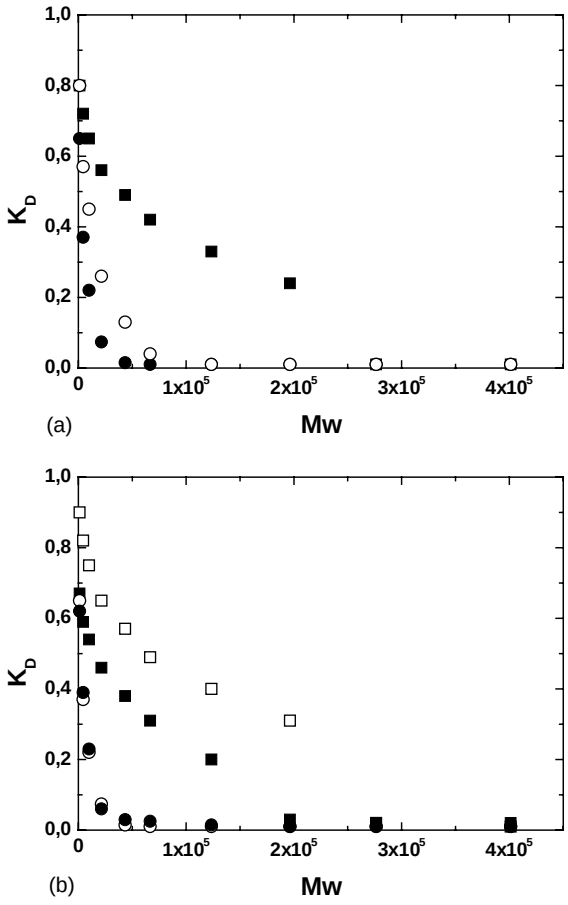

Fig. 2. Distribution coefficients K_D for various molecular weight standards obtained for SP Sepharose™ FF and SP Sepharose™ XL. Dextran standards ranging from 1.08 to 401.3 kg/mole were used. Key: (a) (■) SP Sepharose™ FF; (●) SP Sepharose™ XL; (○) SP Sepharose™ XL (1 M NaCl); (b) SP Sepharose™ FF prior (□) and after (■) BSA saturation; SP Sepharose™ XL prior (○) and after (●) BSA saturation.

it is evident that the pore accessibility of SP Sepharose™ XL is under non-binding conditions considerably smaller for high molecular weight dextran standards when compared to SP Sepharose™ Fast Flow. This is attributed to the network of flexible dextran chains present within the pores [21]. The conformation and properties of the 'pore phase' is a complex interplay between the flexibility of the ligand-carrying polymers, the mobile phase, and thus of the repulsion effects arising from neighbouring ion exchange groups. At low ionic strength and thus high Debye length it can be envisaged that the strong interactions between the unshielded sulfopropyl groups might lead to a rather stiff network conformation which is difficult to penetrate for large molecules. When shielding the charges by applying a 1 M NaCl buffer prior to the measurements the obtained K_D values show an increase of pore accessibility for the SP Sepharose™ XL adsorbents indicating a change in the conformation of the ligand-carrying network (see Fig. 2a). The latter might be explained by a higher flexibility of the network due to a lower degree of interaction between the charge carrying chains. The influence of BSA adsorbed prior to the determination of the K_D values is shown in Fig. 2b. During this study, a significant decrease in pore accessibility for the SP Sepharose™ Fast Flow adsorbent could be observed while the pore accessibility of the SP Sepharose™ XL adsorbent was mostly unaffected. The latter might be directly connected to the fact that for the SP Sepharose™ Fast Flow adsorbent BSA binding is restricted to the pore surfaces leading to stiff layer of adsorbed molecules and thus reduced but still accessible pore size while the SP Sepharose™ XL—as a result of the dextran chains filling the pore volume—offers flexible adsorption sites and a significantly increased volumetric space for the adsorbed molecules. When comparing the experimental K_D values for the investigated proteins with the actual capacity of the adsorbent for the respective molecules it has to be noted that the decrease in the pore accessibility for larger solutes is not mirrored by the measured maximum binding capacities for the respective proteins (see Table 1). The viscosity radii for the investigated proteins in this study, BSA and IgG 2a, can be calculated to 3.2 and 4.3 nm, respectively [22]. The solute radius for IgG 2a results in a significant change in the distribution coefficient or statistical average pore accessibility of SP Sepharose™ XL ($K_D \sim 0.05$) when compared to SP Sepharose™ Fast Flow ($K_D \sim 0.55$). Simultaneously we find a significantly higher

Table 1
Adsorption capacity and observed adsorption pattern for the examined conditions

	Adsorbent	SP Sepharose™ FF		SP Sepharose™ XL	
	pH	4.5	5.0	4.5	5.0
BSA	Q_{max} (mg/ml)	172 ± 8.8	137 ± 7.6	200 ± 41.4	132 ± 24.3
	$k_d \times 10^5$ (mM)	0.06 ± 0.021	6.57 ± 1.94	2.24 ± 0.57	26.87 ± 18.36
	Transport mechanism	PD[a]	PD[a]	PD	PD
IgG 2a	Q_{max} (mg/ml)	193 ± 15.5	192 ± 38.4	322 ± 30.6	260 ± 38.7
	$k_d \times 10^5$ (mM)	0.81 ± 0.34	1.15 ± 0.20	0.24 ± 0.11	0.66 ± 0.47
	Transport mechanism	PD[a]	ND[a]	ND	ND
IgG 2a vs. BSA	$Q_{max,IgG}$ (mol)/$Q_{max,BSA}$ (mol)	0.51	0.63	0.73	0.89

PD: pore-diffusive transport mechanism dominant; ND: non-diffusive transport mechanism dominant.
[a] Taken from [14]. The adsorption isotherms have been determined with native (unlabelled) protein.

IgG 2a capacity for the SP Sepharose™ XL adsorbent when compared to SP Sepharose™ Fast Flow (see Table 1). This discrepancy might be explained by the fact that K_D values do not reflect the actual effective pore volume available for a solute under retaining conditions using a composite support. This is further consistent with a study carried out with Streamline™ Q XL and Streamline™ SP XL and a variety of different proteins. These results indicate that the most important parameter influencing the apparent diffusivity in the XL media was not the size of the respective proteins but rather the properties of the proteins with the matrix surface or 'pore phase' [20].

3.2. Finite bath studies

When investigating BSA adsorption in finite bath studies at pH 4.5 an increase in adsorbent capacity from 172 to 200 mg/ml could be detected when comparing SP Sepharose™ Fast Flow and SP Sepharose™ XL (see Table 1 and Fig. 3). At pH 5.0 both adsorbents showed a significantly lower but similar capacity. The higher adsorption capacity of the SP Sepharose™ XL adsorbents at pH 4.5 might result from a better accessibility of the sulfopropyl groups in SP Sepharose™ XL as compared to SP Sepharose™ Fast Flow. At pH 5.0, however, a shift of the net charge of the BSA molecule (pI ∼ 4.8) from positive to negative leads to a reduction of this effect. Even though BSA binding to a cation exchanger is reported for this pH value [23,24], binding sites are now restricted to few patches on the protein surface, and the binding capacity is approximately equal on both adsorbents. For the IgG 2a (pI ∼ 6.0) similar capacities of 193 mg/ml and 192 mg/ml were obtained for SP Sepharose™ FF at both pH values. When changing from SP Sepharose™ Fast Flow to

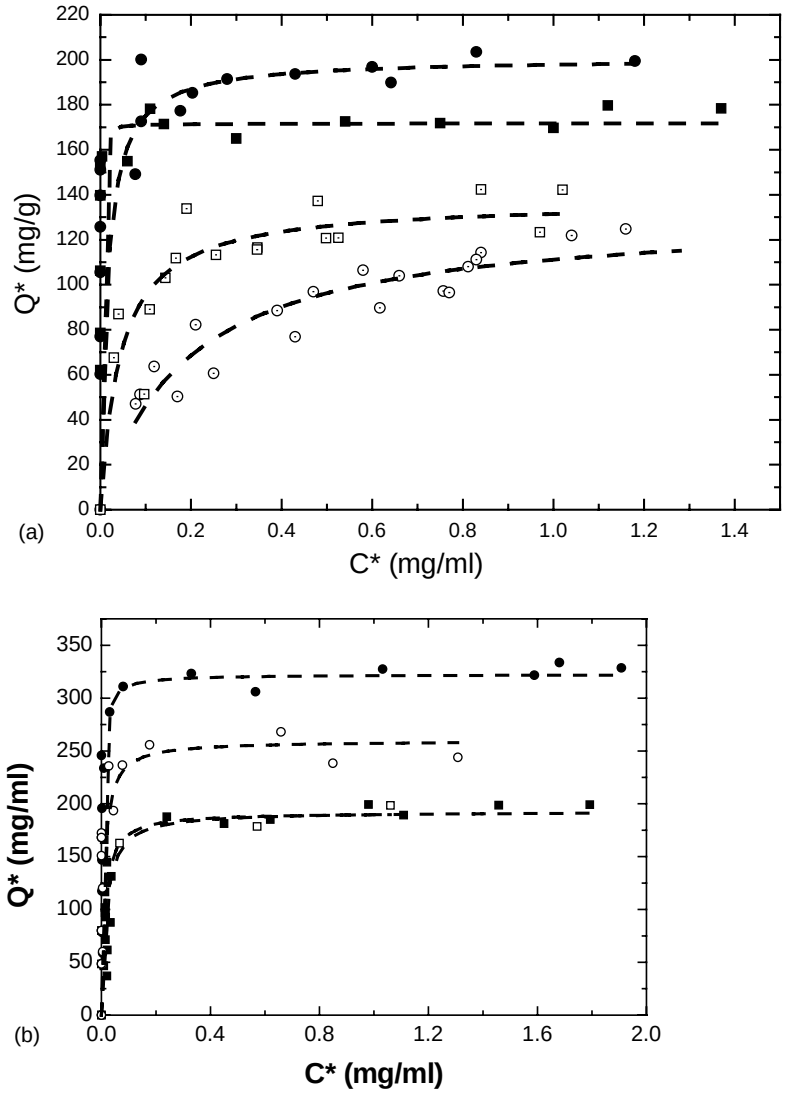

Fig. 3. Adsorption isotherms of (a) BSA and (b) IgG 2a on SP Sepharose™ FF (■, □) and SP Sepharose™ XL (●, ○). Key: (■, ●) pH 4.5; (□, ○) pH 5.0.

SP Sepharose™ XL we, however, found an increase in the sorbent capacity of 67% and 35% at pH 4.5 and 5.0, respectively (see Table 1 and Fig. 3).

This finding is in agreement with studies on a composite resin consisting of a porous silica base matrix filled with polyacrylamide exhibiting a significantly higher capacity than conventional supports [3,4]. A possible explanation for the higher capacities of the SP Sepharose™ XL adsorbent lies in the better accessibility of the ligands. A comparison of the molar capacity—expressed by the ratio of the obtained molar capacities of IgG 2a and BSA—for the investigated supports and the two proteins shows an overall lower capacity for the larger IgG 2a molecule than for BSA (see Table 1). The largest difference in molar capacities was detected for SP Sepharose™ Fast Flow where the molar capacity of IgG 2a was found to be 51% of the molar capacity for BSA at pH 4.5. For SP Sepharose™ Fast Flow pH 5.0 and SP Sepharose™ XL pH 4.5 the ratio reached 63% and 73%, while a surprisingly small difference of only 11% was obtained for SP Sepharose™ XL at pH 5.0.

The saturation kinetics of BSA and IgG 2a for the different systems are shown in Fig. 4. The saturation rate for BSA is different for the two adsorbents. The open pore structure of SP Sepharose™ Fast Flow results in fast uptake kinetics resulting in 90% saturation at approximately 378 and 287 min for pH 4.5 and 5.0, respectively. It is shown in Fig. 2b that the adsorption of BSA leads to a significant decrease in the K_D value of the Fast Flow adsorbent. It can be expected that this effect might be closely linked to the amount of BSA adsorbed. The faster transport and faster saturation at pH 5.0 might therefore be connected to a better pore accessibility due to a lower steric hindrance of molecules being transported into the adsorbent and an overall lower adsorbent capacity when compared to pH 4.5 (see Table 1 and Fig. 3). The SP Sepharose™ XL adsorbent with significantly lower K_D values reached 90% BSA saturation after 880 min and 1245 for pH 4.5 and 5.0, respectively. In contrast to data for the SP Sepharose™ Fast Flow adsorbent, the K_D value for solutes on SP Sepharose™ XL adsorbent is rather independent of BSA adsorbed to the support, in the tested size range (Fig. 2b). The actual conformation of the ligand-carrying layer of the SP Sepharose™ XL adsorbent can, however, be expected to depend on fluid phase conditions or a change of the interactions—binding strength, binding sites—between the ligand-carrying dextran chains and the respective proteins.

The fastest saturation of the support is observed for IgG 2a adsorption on SP Sepharose™ XL at pH 5.0 (90% at ~85 min) (see Fig. 4). This finding further indicates an accelerated overall transport of IgG 2a when compared to the results obtained with BSA, especially considering that the maximum binding capacities for this adsorbent are comparable. Furthermore, it can be seen from Fig. 4b that the obtained sorption kinetics can be divided into three groups. The fastest saturation was found for SP Sepharose™ XL

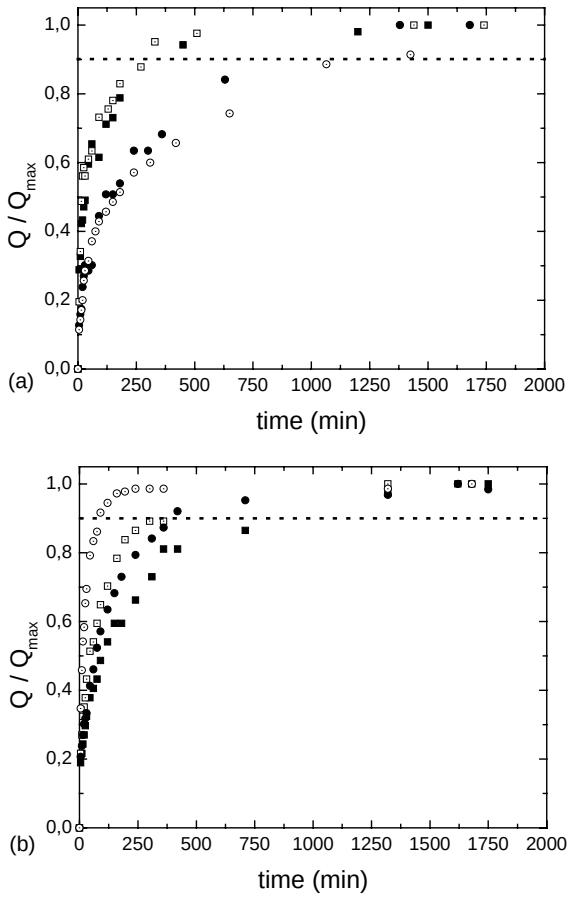

Fig. 4. Kinetic evaluation of (a) BSA and (b) IgG 2a adsorption on SP Sepharose™ FF (■ ⊡), and SP Sepharose™ XL (●, ⊙) employing a 1 mg/ml protein solution. Key: (■, ●) pH 4.5; (⊡, ⊙) pH 5.0.

at pH 5.0, while near identical saturation kinetics are observed for both SP Sepharose™ Fast Flow at pH 5.0 and SP Sepharose™ XL at pH 4.5 with an 90% saturation at 364 and 396 min, respectively. The slowest saturation is found for SP Sepharose™ Fast Flow at pH 4.5 with 932 min for 90% saturation. While the results obtained for BSA might be explained by simple considerations of pore accessibility, the complex interplay between mobile and stationary phase conditions clearly points towards a dominating protein transport mechanism for IgG 2a, which is different to that of BSA under the experimental conditions studied.

3.3. Adsorption profiles

Adsorption profiles of the single component systems were evaluated employing confocal laser scanning microscopy paired with a multi-dye method developed by Linden et al. [14]. This procedure does not only provide the net adsorption profiles as previously shown [12,13] but allows conclusions about further desorption and transport of initially adsorbed proteins. From previous studies [14,15] and results presented in the present paper (Figs. 5–7) different dominating transport mechanism can be noted regarding the examined

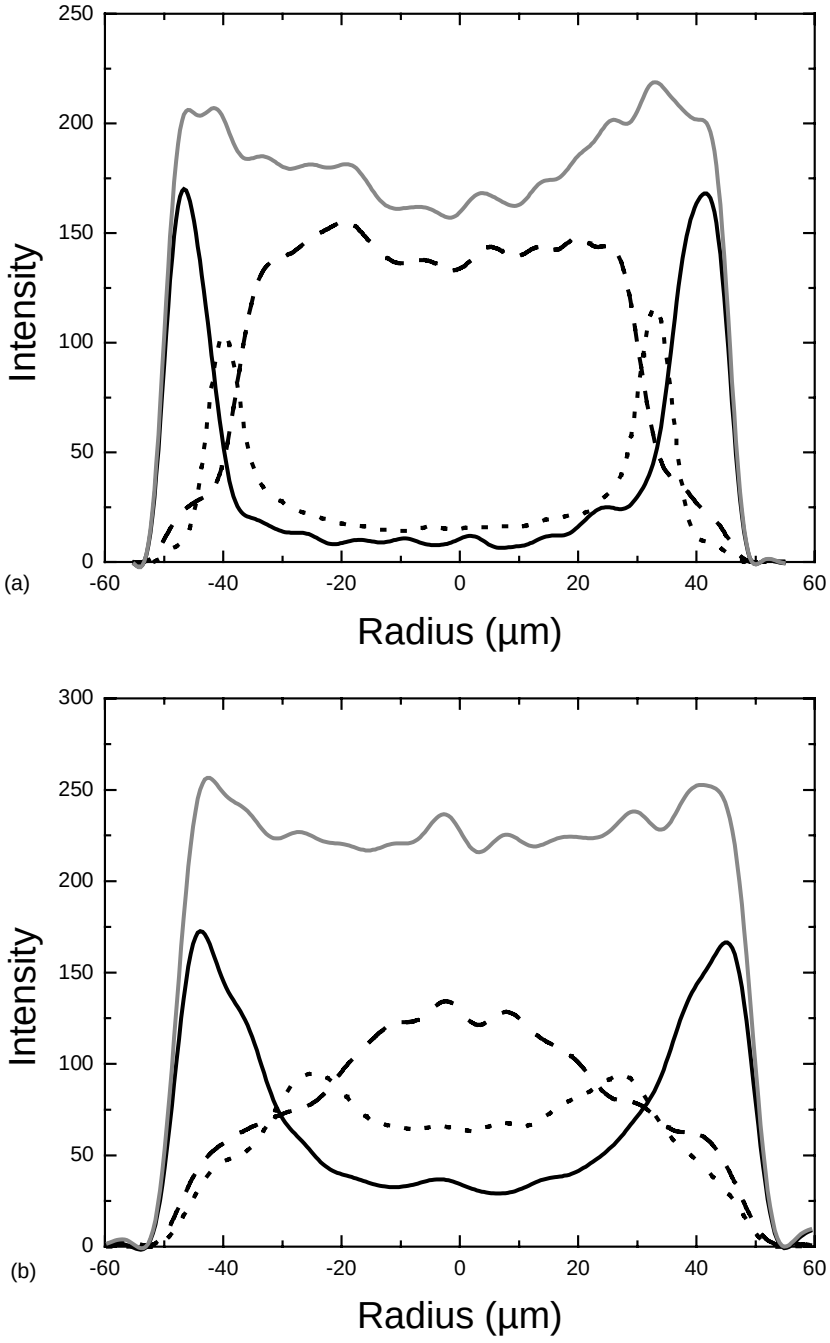

Fig. 5. Adsorption profiles for BSA on SP Sepharose^{TM} XL at near support saturation employing a multi-dye method (batch mode). The adsorbent was incubated with the differently labelled proteins in the following order: ——/·····/– – – and the sum of the respective fluorescent intensities shown as a grey line (——). Conditions: (a) pH 4.5, (b) pH 5.0. The adsorption profiles were smoothed over 10 data points using an FFT function.

systems (see Table 1). Linden et al. [14] investigated the adsorption mechanism of BSA and IgG 2a on SP Sepharose^{TM} Fast Flow at pH 4.5 and 5.0. At an ionic strength identical to the present study, it was found by the authors [14] that BSA adsorption could be described as a gradual filling of the adsorbent from the outmost region towards the center of the support with pore diffusion as the governing transport mechanism. Similar concentration profile development was found for BSA and SP Sepharose^{TM} XL during the present study. Fig. 5 shows the obtained adsorption profiles during BSA adsorption. At pH 4.5 it can be clearly seen that the sorbent has been saturated from the outer rim towards the center exhibiting a sharp adsorption front and that adsorbed protein remained at its initial adsorption site while newly arriving molecules have to be transported past the adsorbed layer to the inner part of the adsorbent. This transport and adsorption behaviour might thus be described by the pore diffusion mechanism occurring under favourable binding

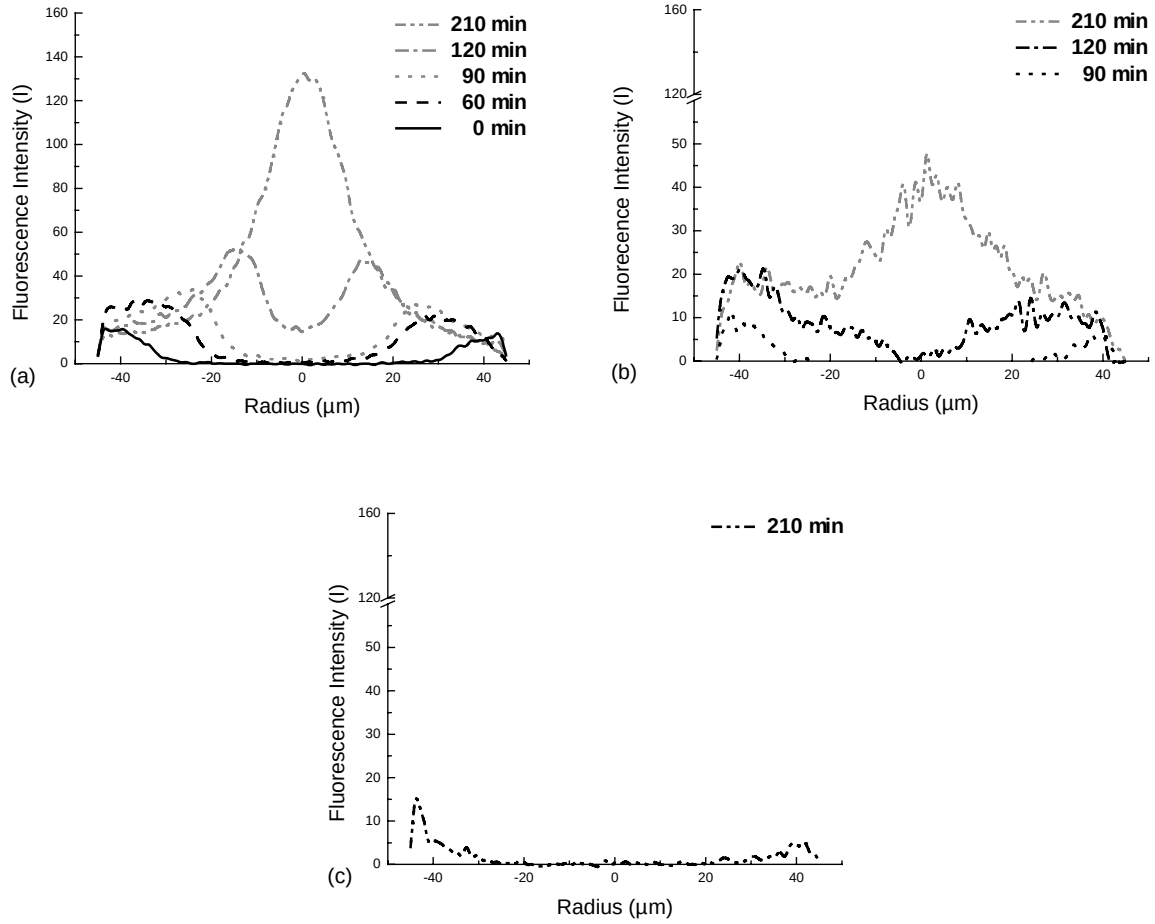

Fig. 6. Adsorption profiles for IgG 2a on SP Sepharose^{TM} XL at pH 4.5 evaluated with the multi-dye method (Column mode). The dynamic profile development was detected employing the micro-column. The supports were incubated in the following order (a) IgG-Cy5; (b) IgG-Alex 488^{TM}; (c) IgG-Cy3. A switch from black to grey symbols indicates a switch to the next feed solution, i.e. further adsorption profiles (grey symbols) describe transport of initially adsorbed protein. The adsorption profiles were smoothed over 10 data points using an FFT function.

conditions producing a self-sharpening effect of adsorbing front inside the particle. The more shallow adsorption front at pH 5.0 reflects the higher dissociation constant found for these conditions (see Table 1) and is consistent with studies carried out under mobile phase conditions with higher ionic strength and thus lower binding strength [14]. Generally, an increase in protein desorption and further transport with a decrease in binding strength of a protein species to the respective solid phase sorbent has been detected for both adsorbents investigated in this study.

During the evaluation of IgG 2a adsorption the behaviour described above could only be observed for adsorption at pH 4.5 on SP Sepharose^{TM} Fast Flow. It was shown in a previous study [14] that a change in the mobile phase conditions from pH 4.5–5.0 leads to a significant change in the transport behaviour detected for IgG 2a on SP Sepharose^{TM} Fast Flow. The dynamics of protein adsorption and transport under these conditions could be described as a ‘wave’ of molecules building up towards the inner section of the support and leading to an overshoot in the centre of the particle. The accumulation is only temporary as it is followed by a return to equilibrium, where a homogeneous sorption profile of the differently labelled protein fractions was established [15]. While this overshoot behaviour was not shown in the previous work [14], the homogeneous distribution of the different dye fractions at saturation obtained when using the multi-dye method corresponds to the profile development found when the overshoot behaviour has been detected in the present study. Somewhat, similar concentration profile development has earlier been reported by Ljunglöf [25], Linden [26] and Dziennik [18] during their investigations of protein adsorption on cation exchange adsorbents.

The adsorption profiles obtained for SP Sepharose^{TM} XL at pH 4.5 resembles the transport dynamics found for SP Sepharose^{TM} Fast Flow at pH 5.0 as described above (i.e. [15]) (see Fig. 6a–c). The respective evaluation employing the multi-dye method (see Section 2.9) has been carried out in a microcolumn by switching the feed solution from IgG-Cy5 to IgG-Alexa 488^{TM} and IgG-Cy3. In order to resolve the dynamics of protein uptake we plotted the development of the intensity profiles of the differently labelled fractions detected within a single support particle beneath

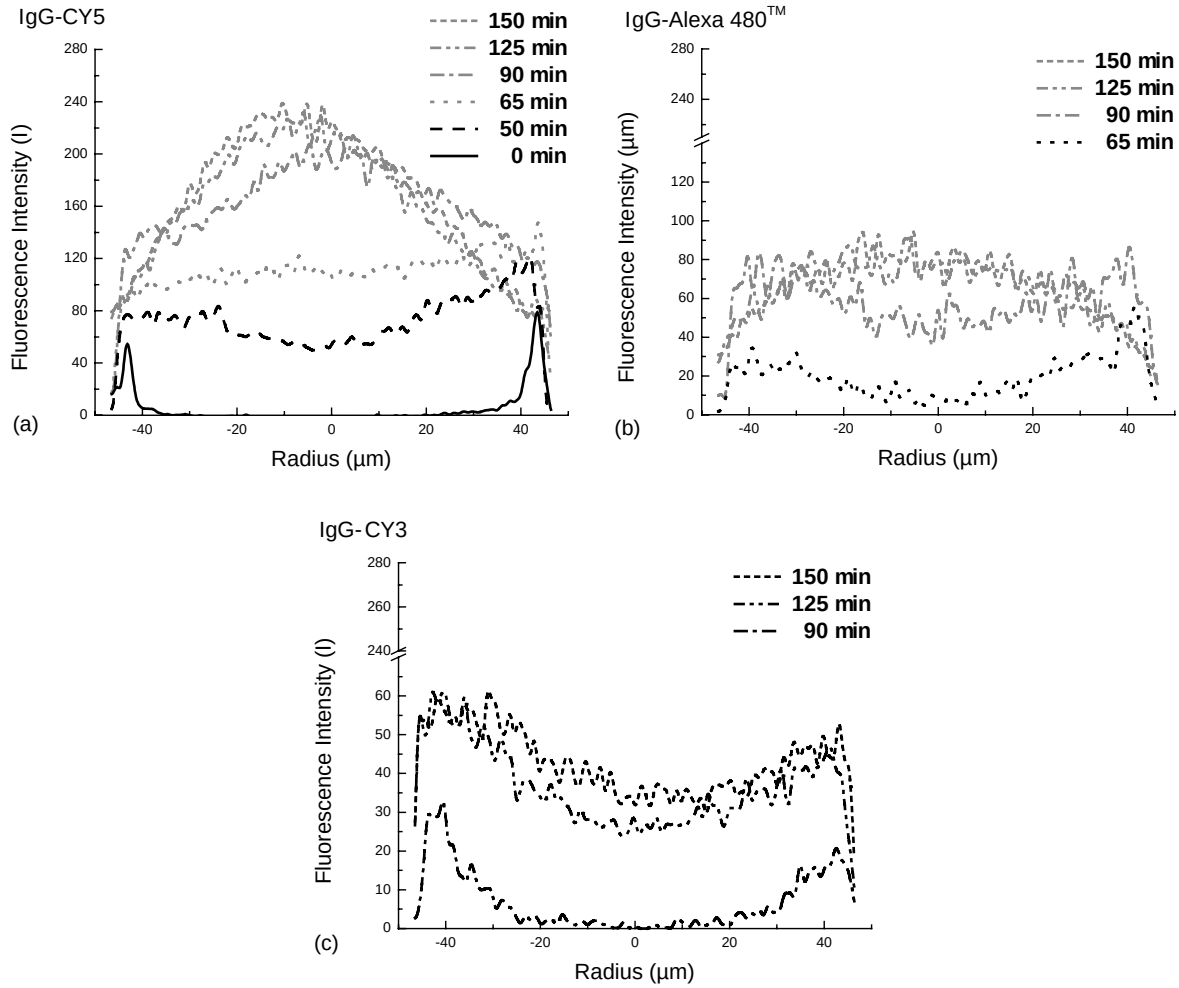

Fig. 7. Adsorption profiles for IgG 2a on SP Sepharose^{TM} XL at pH 5.0 evaluated with the multi-dye method (Column mode). The dynamic profile development was detected employing the micro-column. The supports were incubated in the following order (a) IgG-Cy5; (b) IgG-Alex 480^{TM}; (c) IgG-Cy3. A switch from black to grey symbols indicates a switch to the next feed solution, i.e. further adsorption profiles (grey symbols) describe transport of initially adsorbed protein. The adsorption profiles were smoothed over 10 data points using an FFT function.

each other. The symbols in Fig. 6a–c further change from closed (black) to open (grey) symbols after the feed has been switched to the next feedstock. The new feed fractions adsorb to the support, i.e. the development of the graphs with open symbols in the respective plots (a–c) in Fig. 6 represents the transport of initially accumulated or adsorbed protein only. Initially the adsorption front of IgG-Cy5 is building up leading to a saturation of the outer shells of the support (Fig. 6a). In the meantime the feed has been switched from IgG-Cy5 to IgG-Alexa 488^{TM} and initial binding of IgG-Alexa 488^{TM} was detected after 90 min. Any additional development of the IgG-Cy5 adsorption profile is therefore based on further transport and adsorption of IgG-Cy5 molecules initially accumulated and adsorbed during the first ~60 min (Fig. 6a). It is evident that part of IgG-Cy5 bound at the outer rim of the support is transported to the inner part of the sorbent. This behaviour leads to a decrease of the intensity at the outer shell and the development of a 'wave'-like profile at the inner section of the support before resulting in an overshoot in the center of the support after 210 min. As the IgG-Cy5 is transported to the inner part of the adsorbent particle, the newly arriving IgG-Alexa 488^{TM} is binding to the outside of the support (90, 120 min). Meanwhile, a second change of the feed has been carried out and Fig. 6c shows again that newly arriving protein (IgG-Cy3) initially binds at the outer rim of the support (210 min). The adsorbed IgG-Alexa 488^{TM} is now—similar to the IgG-Cy5 adsorption front—transported to the centre of the support as seen for IgG-Cy5. The overshoot developed after 210 min is, however, smaller than detected with IgG-Cy5. At equilibrium, the overshoot is set back to an equilibrium level resembling approximately the intensity found in Fig. 6a after the first 60 min (data not shown). The latter is consistent with the adsorption front development found for IgG 2a adsorption on SP Sepharose^{TM} Fast Flow at pH 5.0 [15].

The same methodology was used to investigate IgG 2a adsorption on Sepharose^{TM} XL at pH 5.0 and the respective plots are shown in Fig. 7a–c. The change of mobile phase

conditions from pH 4.5–5.0 did not lead to a 'wave' like formation but resulted in a homogeneous adsorption front over the whole particle radius within 50 min (see Fig. 7a). After 65 min the initial adsorption front of IgG-Alexa 488™ is detected in Fig. 7b and it becomes evident that this adsorption front is immediately spread over the cross sectional area of the support. The pictures taken at 90, 125 and 150 min show that the homogeneous adsorption front of IgG-Cy5 is indicating some sort of overshoot. The relative magnitude is greatly reduced when compared to the adsorption profiles found at pH 4.5. The adsorption profiles obtained with the third feed fraction IgG-Cy3 show again that newly approaching molecules are initially bound at the outside of the sorbent before covering the whole cross sectional area of the support.

4. Summary and conclusions

A detailed experimental study of protein transport has been carried out, including different adsorbent structures, proteins and mobile phase conditions. The data obtained by traditional fluid phase measurements (adsorbent capacity, saturation kinetic) were supplemented by the evaluation of adsorption profiles in single component systems employing confocal laser scanning microscopy. For the investigated systems, transport and adsorption of BSA to SP Sepharose™ XL could be approximated by the pore diffusion mechanism occurring under conditions of favourable adsorption isotherm and showed consistent behaviour found for BSA adsorption on SP Sepharose™ Fast Flow during earlier studies [14]. This conclusion was drawn based on the adsorption profiles obtained with the multi-dye method. For IgG 2a adsorption to Sepharose™ XL, a more complex transport/adsorption behaviour has been noticed. Regardless of the low K_D values found for IgG 2a and SP Sepharose™ XL, we detected high capacities and the overall fastest saturation of the sorbent, which indicates a significant contribution of a possibly non-diffusive mechanism to protein transport.

The results obtained in this study and in the earlier work [14] indicate that the governing/predominant mechanism behind protein transport in ion exchange adsorbents depends on mobile phase composition, protein properties and, also, on adsorbent intraparticle structure. Under certain conditions, the predominant mechanism will have non-diffusive character and may result in a significantly faster transport and therefore saturation of the sorbent. Furthermore, under certain conditions a phenomena of a protein overshoot inside adsorbent particle can be observed. Liapis et al. [16] gave a mechanistic explanation for the 'overshoot' behaviour by considering electrostatic potential distribution within pore of the adsorbent particles and its effects on mass transfer by diffusion, electrophoretic migration and adsorption of protein as well as the supporting electrolyte. This was further outlined by Grimes and Liapis [17] who showed how the interplay of diffusive and electrophoretic transport mechanisms will affect functioning of the electrical double layer present inside pores of charged adsorbent particles that could contribute to the 'overshoot' behaviour. Recently, Dziennik et al. [18] discussed an electrokinetic contribution to the transport in ion exchange particle and found that the 'overshoot' effect could be correlated to high adsorbent surface charge densities. The results presented in this work showed that a detailed understanding of the parameters describing the mobile and stationary phases might be utilized for optimization of chromatographic separations based on the governing mass transport mechanism. First implications for chromatographic protein separation based on the forementioned principle will be evaluated and discussed in a following paper.

Acknowledgements

The authors acknowledge the German Research Society (DFG) for funding this project (TH 702/1-1; 1-2). The authors thank Dr. Lars Hagel at Amersham Biosciences AB for valuable comments to the manuscript.

References

[1] J. Bonnerjea, S. Oh, M. Hoare, P. Dunnill, Bio./Technology 4 (1986) 945.
[2] E. Boschetti, J. Chromatogr. A 658 (1994) 207.
[3] M.A. Fernandez, G. Carta, J. Chromatogr. A 746 (1996a) 169.
[4] M.A. Fernandez, G. Carta, J. Chromatogr. A 746 (1996) 185.
[5] L.E. Weaver, G. Carta, Biotechnol. Prog. 12 (1996) 342.
[6] R.K. Lewus, F.H. Altan, G. Carta, Ind. Eng. Chem. Res. 37 (1998) 1079.
[7] B.H. Arve, A.I. Liapis, AIChE J. 33 (1987) 179.
[8] A. Johnston, M.T.W. Hearn, J. Chromatogr. 557 (1991) 335.
[9] H. Yoshida, M. Yoshikava, T. Kataokal, AIChEJ 40 (1994) 2034.
[10] C. Chang, A.M. Lenhoff, J. Chromatogr. A 827 (1998) 281.
[11] A. Ljunglöf, R. Hjorth, J. Chromatogr. A 743 (1996) 75.
[12] A. Ljunglöf, J. Thömmes, J. Chromatogr. A 813 (1998) 387.
[13] T. Linden, A. Ljunglöf, M.R. Kula, J. Thömmes, Biotech. Bioeng. 65 (6) (1999) 622.
[14] T. Linden, A. Ljunglöf, L. Hagel, M.R. Kula, J. Thömmes, Separat. Sci. Technol. 37 (1) (2002) 1.
[15] J. Hubbuch, T. Linden, E. Knieps, J. Thömmes, M.R. Kula, Biotechnol. Bioeng. 80 (4) (2002) 359.
[16] A.I. Liapis, B.A. Grimes, K. Lacki, I. Neretnieks, J. Chromatogr. A 921 (2) (2001) 135.
[17] B.A. Grimes, A.I. Liapis, J. Colloid Intref. Sci. 248 (2002) 504.
[18] S.R. Dziennik, E.B. Belcher, G.A. Barker, M.J. DeBergalis, S.E. Fernandez, A.M. Lenhoff, PNAS 100 (2) (2003) 421.
[19] C. Martin, G. Iberer, A. Ubiera, G. Carta, ISPPP 2002, 10–13 November, Heidelberg, 2002.
[20] J. Thömmes, Biotechnol. Bioeng. 62 (3) (1999) 358.
[21] L. Hagel, in: M. Potschka, P.L. Dubin (Eds.), Strategies in Size Exclusion Chromatography (ACS Symposium Series 635), American Chemical Society, Washington, DC, 1996, pp. 225–248.
[22] L. Hagel, in: J.C. Janson, L. Ryden (Eds.), Protein Purification, Principles, High Resolution Methods and Applications, Wiley-VCH, New York, 1998, pp. 79–144.

[23] W. Kopaciewicz, M.A. Rounds, J. Fausnaugh, F.E. Regnier, J. Chromatogr. 266 (1983) 3.
[24] G.L. Skidmore, B.J. Horstmann, H.A. Chase, J. Chromatogr. 498 (1990) 113–128.
[25] A. Ljunglöf, Doctoral thesis, Direct observation of biomolecule adsorption and spatial distribution of functional groups in chromatographic adsorbent particles, Uppsala University 2002, http://www.uu.se/avhandlingar.
[26] T. Linden, Doctoral thesis, Untersuchungen zum inneren Transport bei der Proteinadsorption an poröse Medien mittels konfokaler Laser-Raster-Mikroskopie, Heinrich-Heine-Universität Düsseldorf, 2001.